



Heriot-Watt University
Research Gateway

Transient Optical Properties of CsPbX₃/Poly(maleic anhydride-alt-1-octadecene) Perovskite Quantum Dots for White Light-Emitting Diodes

Citation for published version:

Xu, J, Zhu, L, Chen, J, Riaz, S, Sun, L, Wang, Y, Wang, W & Dai, J 2021, 'Transient Optical Properties of CsPbX₃/Poly(maleic anhydride-alt-1-octadecene) Perovskite Quantum Dots for White Light-Emitting Diodes', *Physica Status Solidi - Rapid Research Letters*, vol. 15, no. 1, 2000498.
<https://doi.org/10.1002/pssr.202000498>

Digital Object Identifier (DOI):

[10.1002/pssr.202000498](https://doi.org/10.1002/pssr.202000498)

Link:

[Link to publication record in Heriot-Watt Research Portal](#)

Document Version:

Peer reviewed version

Published In:

Physica Status Solidi - Rapid Research Letters

Publisher Rights Statement:

This is the peer reviewed version of the following article: Xu, J., Zhu, L., Chen, J., Riaz, S., Sun, L., Wang, Y., Wang, W. and Dai, J. (2021), Transient Optical Properties of CsPbX₃/Poly(maleic anhydridealt1octadecene) Perovskite Quantum Dots for White LightEmitting Diodes. *Phys. Status Solidi RRL*, 15: 2000498, which has been published in final form at <https://doi.org/10.1002/pssr.202000498>

This article may be used for non-commercial purposes in accordance with Wiley Terms and Conditions for Use of Self-Archived Versions.

General rights

Copyright for the publications made accessible via Heriot-Watt Research Portal is retained by the author(s) and / or other copyright owners and it is a condition of accessing these publications that users recognise and abide by the legal requirements associated with these rights.

Take down policy

Heriot-Watt University has made every reasonable effort to ensure that the content in Heriot-Watt Research Portal complies with UK legislation. If you believe that the public display of this file breaches copyright please contact open.access@hw.ac.uk providing details, and we will remove access to the work immediately and investigate your claim.

Transient Optical Properties of CsPbX₃/maleic anhydride-alt-1-octadecene Perovskite Quantum Dots for White Light-Emitting Diodes

Jian Xu¹, Liang Zhu¹, Jia Chen², Saba Riaz¹, Liwei Sun¹, Ying Wang¹, Wei Wang³, * Jun Dai¹, *

¹ Department of Physics, Jiangsu University of Science and Technology, Zhenjiang, 212003, China.

² Jolywood solar technology co. ltd, Research and Development Department, Taizhou, 225500, China.

³ School of Engineering and Physical Science, Heriot-Watt University, Edinburgh, EH14 4AS, United Kingdom

E-mail: daijun@just.edu.cn

Received xxxxxx

Accepted for publication xxxxxx

Published xxxxxx

Abstract

The polymer PMAO (maleic anhydride-alt-1-octadecene) with its long hydrophobic alkyl chain bound to the surface ligands of perovskite and act as a protective layer. Time-resolved photoluminescence (TRPL) shows that the photoluminescence lifetime of CsPbX₃/PMAO is prolonged, and the transient absorption (TA) results show that intraband hot-exciton relaxation and exciton recombination can be slowed down when the CsPbX₃ is coated with PMAO. White light-emitting diode devices are fabricated by integrating the green CsPbBr₃/PMAO quantum dots (QDs) and red CsPbBr_{1.6}I_{1.4}/PMAO QDs on the blue GaN chips with Commission Internationale de L'Eclairage color coordinates of (0.314, 0.291).

Keywords: quantum dots, perovskite, white light-emitting diodes

Lead halide perovskite materials attract tremendous attention for their promising applications in optoelectronic devices¹⁻⁵. Among them, all-inorganic metal halide perovskite (CsPbX₃, X=Cl, Br, I) QDs present higher photoluminescence quantum yields (PLQYs), narrower photoluminescence linewidth, and better stability than organic-inorganic hybrid perovskite CH₃NH₃PbX₃ (X = Cl, Br, I)⁶⁻⁹. Researchers have made significant improvements in optimizing the physical properties of CsPbX₃, such as increasing its quantum efficiency and stability, and also the photoluminescence mechanism was investigated¹⁰⁻¹². Now the external quantum efficiency of CsPbBr₃ based LEDs has been increased from 0.12% to 22%^{7, 13}. However, the perovskite QDs are sensitive to air and humidity, which limits their practical commercial applications^{4, 14}. Recently, some strategies were used to enhance the stability of perovskite QDs, such as compositional engineering^{15, 16}, surface engineering¹⁷, and encapsulation engineering¹⁸⁻²⁰. Encapsulating the perovskite QDs with

transparent dielectrics is a feasible approach for realizing high stability²¹. Chen et al. prepared CsPbMnCl₃ QDs encapsulated in silicon dioxide (SiO₂), and use it as down-conversion orange-red luminescent materials on the blue LED chip to get the white light emission²². Recently, the researchers found that PMAO coated CsPbBr₃ perovskite QDs can improve the stability and also passivate the surface defect of the perovskite QDs. Yang's group reported the white-light emitting device by integrating the green CsPbBr₃/PMAO QDs and organic red luminescent phosphor on the blue LED chips²⁰. Meyns et al. and Liu et al. reported the white LED based on the green CsPbBr₃/PMAO and orange-red CsPbBr_{1.6}I_{1.4}/PMAO perovskite QDs, respectively^{19, 23}. However, the CsPb (Br/I)₃/PMAO presents a photoluminescence wavelength center at 620 nm, which is orange-red but not standard red. The standard red light covers the wavelength from 625 to 770 nm, the red CsPbX₃ QDs with PMAO surface passivation (660 nm) has not been reported in the white light-emitting devices. More importantly, the

transient absorption and transient photoluminescence of the PMAO coated CsPbX₃ are not systematically studied to reveal the dynamic process of carrier, and the effect of the coating layer PMAO on the optical process is not clear.

In this work, we synthesized PMAO-coated green CsPbBr₃ QDs and red CsPbBr_{1.2} QDs. The femtosecond transient absorption (TA) and time-resolved photoluminescence (TRPL) of the CsPbBr₃/PMAO and CsPbBr_{1.2}/PMAO perovskite QDs were studied, the photoluminescence recombination process and exciton excitation process were revealed, the result indicates that surface defects of CsPbBr₃ and CsPbBr_{1.2} QDs were reduced after PMAO coating. The blue GaN chip was employed to excite the green CsPbBr₃/PMAO layer and red CsPbBr_{1.2}/PMAO QDs layer, and the stable white light emission can be obtained.

Figure 1(a-b) show the transmission electron microscopy (TEM) images and size distribution of CsPbBr₃/PMAO and CsPbBr_{1.2}/PMAO QDs. The experimental methods could be

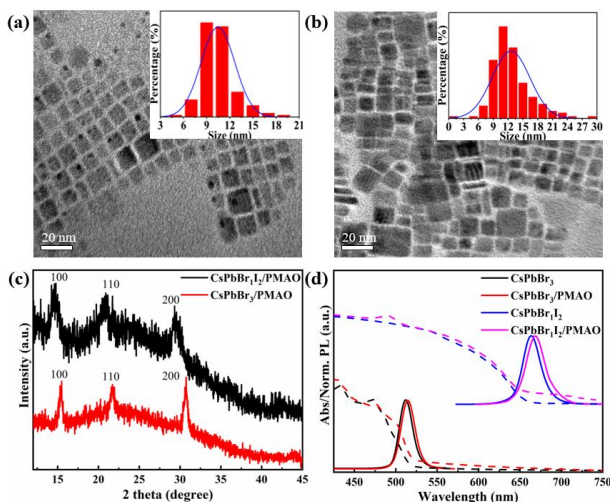


Figure 1. TEM images of (a) CsPbBr₃/PMAO, (b) CsPbBr_{1.2}/PMAO. The insets represent the corresponding size distribution histograms. (c) XRD pattern of CsPbBr₃/PMAO and CsPbBr_{1.2}/PMAO QDs. (d) Comparison of the absorption spectrum (dash line) and PL spectrum (solid line) of CsPbBr₃ and CsPbBr_{1.2} with and without the PMAO layer.

seen in the supplementary data. All the samples exhibit a stable cubic phase structure with an orderly arrangement. The average sizes were 10.5 nm and 12.6 nm for CsPbBr₃/PMAO and CsPbBr_{1.2}/PMAO, respectively. Figure 1c shows the X-ray diffraction (XRD) patterns of CsPbBr₃/PMAO and CsPbBr_{1.2}/PMAO QDs. The (100), (110), and (200) crystal plane diffraction peaks of these two types of QDs were observed, which indicates these two samples present typical cubic phase structures. Compared with CsPbBr₃/PMAO QDs, the diffraction peaks of red perovskite CsPbBr_{1.2}/PMAO QDs present a smaller angle shift for its larger lattice constant. Figure 1d shows the UV-Vis absorption spectrum and photoluminescence (PL) spectrum of QDs with and without

the PMAO layer. Compared with pristine CsPbBr₃ and CsPbBr_{1.2} QDs, no defect-related absorption and PL peaks can be found for the two types of PMAO-coated samples, and the PL emission wavelength of the PMAO-coated QDs show a slight redshift, which is related to the larger size.

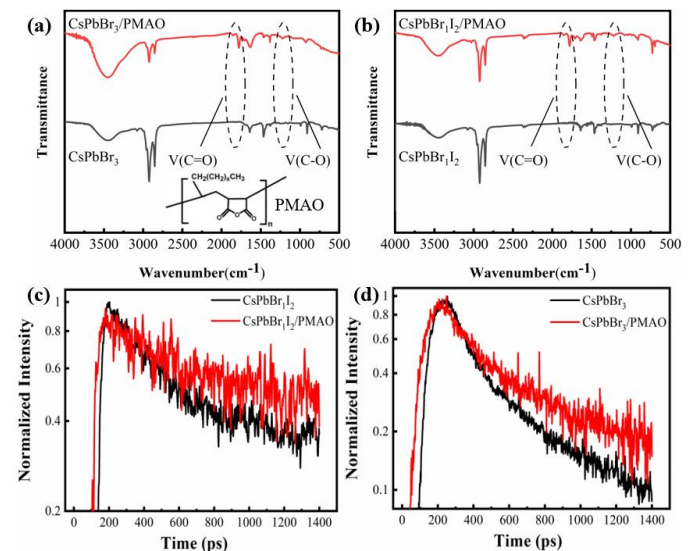


Figure 2. FTIR spectrum of as-prepared (a) CsPbBr₃/PMAO and (b) CsPbBr_{1.2}/PMAO QDs. The illustration in Figure 2a is the chemical structure of PMAO. Time-resolved PL decay curves of (c) CsPbBr₃ and CsPbBr₃/PMAO QDs (d) CsPbBr_{1.2} and CsPbBr_{1.2}/PMAO QDs.

The Fourier Transform Infrared Spectroscopy (FTIR) of CsPbBr₃/PMAO and CsPbBr_{1.2}/PMAO QDs in Figure 2(a-b) show the characteristic signals of stretching vibrations of C=O located at ~1859 and ~1780 cm⁻¹, and C-O stretching vibration at ~1222 cm⁻¹. The C=O and C-O stretching vibrations originate from the anhydride group of the PMAO polymer, which indicates the effect coating of the PMAO polymer on the surface of perovskite QDs. Time-resolved photoluminescence (TRPL) spectroscopy is depicted in Figure 2(c-d), the average lifetime of CsPbBr₃/PMAO (273.48ps) and CsPbBr_{1.2}/PMAO (434.57ps) is longer than that of pristine CsPbBr₃ (206.96ps) and CsPbBr_{1.2} (294.72ps). Longer PL decay time reveals the reduction of nonradiative decay rate, which indicates that the PMAO polymer can act as a surface passivation layer and reduces the nonradiative decay pathways for the exciton.

To better understand the photophysical essence of the PMAO coated perovskite QDs, the ultrafast transient absorption (TA) was conducted using a pump laser at 365 nm. Excitation power density (2.0×10^{14} photons/cm²/pulse) is kept a low level to avoid the formation of biexcitons and multiexcitons in the CsPbBr₃/PMAO and CsPbBr_{1.2}/PMAO QDs. As shown in Figure 3a-b, the transient absorption spectrum of the CsPbBr₃/PMAO QDs has three peaks: (a) Photo bleaching (PB) peak at 518nm, $\Delta A < 0$. It shows that the decrease in the number of ground-state electrons and the

increase in the number of excited-state electrons leads to a decrease in the optical absorption of the detector light. (b) Photo absorption (PA1) peak at 450-510nm, $\Delta A > 0$. It appears that the sample's absorption of the probe light is increased, which is caused by the absorption of the lowest excited state. (c) Short-lived absorption peak (PA2) at 534nm. The optical bandgap and the ground state bleaching peak are agreed with the reference²⁴. The ground state bleaching signal peak position at 518nm (corresponding to the band gap ~ 2.39 eV) indicates the PMAO does not affect the optical bandgap of CsPbBr₃ QDs.

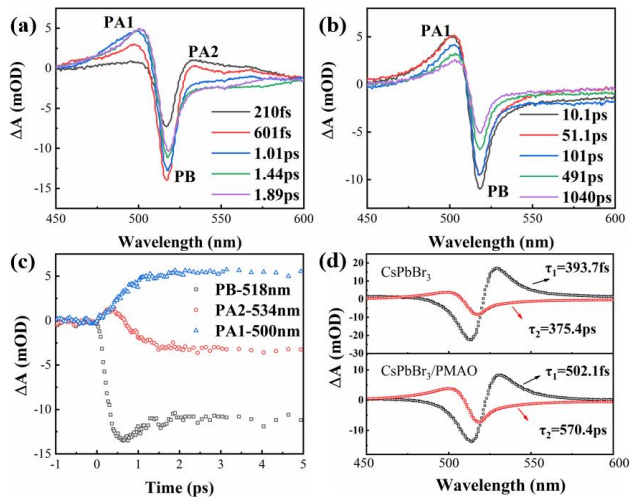


Figure 3. Time-dependent evolution of the TA spectra of CsPbBr₃/PMAO QDs in the (a) (210fs–1.89 ps), (b) (10.1ps–1040 ps) time scales. (c) Evolution of three characteristic signals within 5 ps of CsPbBr₃/PMAO QDs. (d) decay-associated spectra (DAS) for the CsPbBr₃ and CsPbBr₃/PMAO QDs.

Figure 3c presents the evolution of PB, PA1 and PA2 within the first 5 ps. When the femtosecond laser excitation pulse generates excitons above the band gap, the rise of the PB signal in the initial few hundred femtoseconds can be attributed to the transition of electrons from the valence band to the conduction band by absorbing the excitation photons, causing a reduction in the number of ground state excitons. Then these thermal excitons are cooled to band-edge exciton states (in-band relaxation), causing the PB signal to drop²⁵. Different from the lowest exciton state absorption of PA1, the short-lived PA2 is attributed to the hot-exciton absorption, and its decay time (690 fs) matches the formation time of PB. PA1 and PB peaks show a slight redshift in the first few picoseconds, which was owing to the exciton–exciton interaction²⁶. The singular value decomposition (SVD) and global fitting were further used to analyse the TA spectrum of the CsPbBr₃/PMAO. As shown in Figure 3d, two main components were obtained by SVD, the time constants of the two components of the CsPbBr₃/PMAO are $\tau_1 = 502.1$ fs and $\tau_2 = 570.4$ ps. τ_1 and τ_2 are the time of the intraband hot-exciton relaxation and exciton recombination, respectively²⁷. τ_1 is associated with PA2, while τ_2 is

associated with both PA1 and PB bands. The global fitting shows that PMAO will slow down the two processes. Here the prolonged time constants can be due to the decrease in the surface defects of CsPbBr₃ QDs resulting from the effective PMAO coating by van der Waals interaction²⁰. The reduction of shallow level defects may increase the hot-exciton relaxation and exciton recombination time.

As shown in figure 4(a-b), CsPbBr_{1.2}/PMAO QDs show similar spectral features and dynamical parameters to that observed from CsPbBr₃/PMAO QDs. As shown in Figure 6c, the time constants of the two components τ_1 and τ_2 of the CsPbBr_{1.2}/PMAO QDs are 898.9 fs and 421.0 ps. It also shows that with the PMAO layer will make the τ_1 and τ_2 longer, which indicates a reduction in surface defects. However, a distinct redshift of the PB band in the early time (<5 ps) can be distinguished for CsPbBr_{1.2}/PMAO QDs. Figure 4d is a schematic illustration of PB redshift of CsPbBr_{1.2}/PMAO QDs, the CB and VB energy levels of CsPbX₃ QDs are

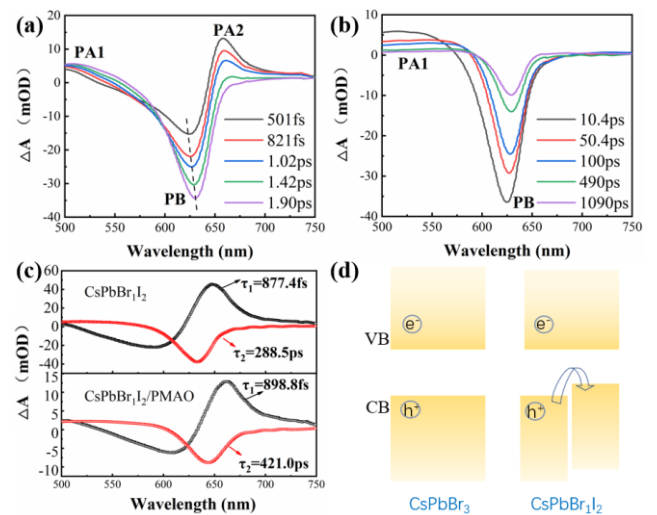


Figure 4. Time-dependent evolution of the TA spectra of CsPbBr_{1.2}/PMAO QDs in the (a) (501 fs–1.9 ps), (b) (10.4 ps–1090 ps) time scales. (c) decay-associated spectra (DAS) for the CsPbBr_{1.2} and CsPbBr_{1.2}/PMAO QDs (d) Schematic illustration of redshift of CsPbBr_{1.2}/PMAO QDs.

sensitive to Pb and X, respectively, and the top of VB is shifted to a higher energy level for CsPbBr_{1.2}²⁸⁻³⁰. Thus, when a mixed halide CsPbBr_{1.2} QDs is excited, the holes created at the Br-site (lower energy level in the VB) can move to the I-site (higher energy level in the VB), which leads to a time-dependent redshift of PB in the first few picoseconds.

As we known, the red perovskite QDs are extremely unstable, here we tested the fluorescence stability of the CsPbBr_{1.2} QDs with and without the PMAO coating layer in the air atmosphere. Figure 5a shows the pictures of CsPbBr_{1.2}/PMAO and CsPbBr_{1.2} QDs spin-coated on a square quartz substrate under a 365 nm UV lamp when they are exposed to the air with a humidity of 80 %, as shown in Figure

5a, the CsPbBr₃/PMAO QDs present much better red fluorescence than the uncoated CsPbBr₃ QDs after being exposed to air for 3 days. So, the PMAO coating can increase the stability of red perovskite QDs. Figure 5b is a schematic diagram of the structure of the White-Light Emitting Diodes (WLED), where the blue GaN-LED chip was employed to

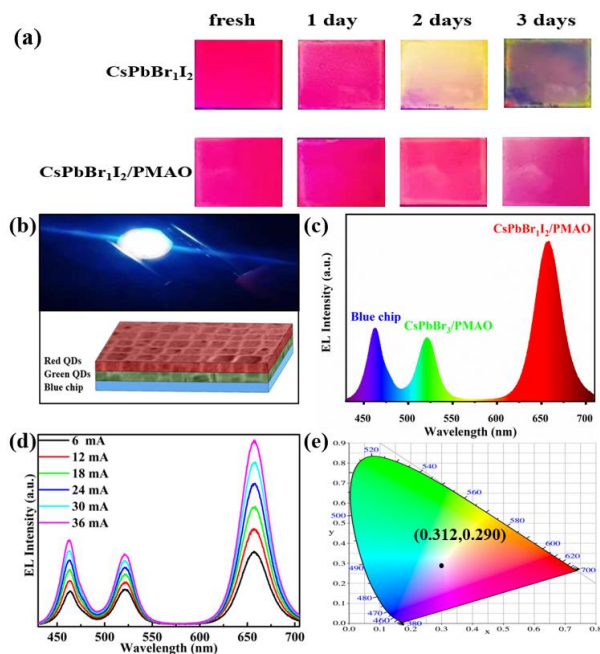


Figure 5. (a) Comparison of stability under air environment of CsPbBr₃I₂ and CsPbBr₃I₂/PMAO QDs. (b) The photograph of WLED operating at 30 mA and schematic diagram of white LED device; (c) EL spectrum of WLED at 30 mA; (d) EL spectrum of WLED under various injection currents of 6-36 mA; (e) CIE colour coordinates of WLED.

excite the green CsPbBr₃/PMAO layer and red CsPbBr₃I₂/PMAO QDs layer. Figure 5c shows the electroluminescence (EL) spectrum of a WLED device at an injection current of 30 mA. It can be observed that the EL spectrum has three emission peaks. The blue emission peak at 460 nm comes from the GaN chip, while the other two emission peaks at 520 nm and 657 nm are from the photoexcited CsPbBr₃/PMAO and CsPbBr₃I₂/PMAO QDs, respectively. No other emission peaks can be observed in the green-red wavelength range, which indicates the absence of an anion exchange reaction between the CsPbBr₃/PMAO and CsPbBr₃I₂/PMAO. Figure 5d shows the EL spectrum of the WLED at different injected currents. The intensity of the three emission peaks increases as the injected current increases, no significant change in spectral shape can be found, which indicates that the EL of the device is stable. The devices show a stable white light emission with Commission Internationale de L'Eclairage (CIE) color coordinates of (0.314,0.291), which is located in the white light area. As a result, the CsPbX₃/PMAO composite can be used as an excellent down-conversion phosphor for WLED devices.

In conclusion, we synthesized the CsPbBr₃/PMAO and CsPbBr₃I₂/PMAO to improve the stability of perovskite QDs. The polymer can act as a steric barrier that helps to inhibit the degradation of QDs caused by external environment. The CsPbBr₃ QDs and CsPbBr₃I₂ QDs after PMAO coated still have a stable cubic phase structure and high fluorescence, and the emission wavelength has not changed significantly. Furthermore, time-resolved photoluminescence and ultrafast transient absorption spectroscopy revealed that the PMAO contributes to passivating surface defect of the CsPbX₃ QDs. Finally, a high-quality WLED with a colour coordinate of (0.314, 0.291) was obtained. The results show that all-inorganic perovskite/PMAO QDs composite has great application potential in the field of luminescence and display.

Acknowledgements

This work was supported by National Science Foundation of China [11874185].

Conflict of Interest

The authors declare no conflict of interest.

References

- 1) N.-G. Park, *The Journal of Physical Chemistry Letters*. **4**,2423 (2013).
- 2) L. Protesescu, S. Yakunin, M.I. Bodnarchuk, F. Krieg, R. Caputo, C.H. Hendon, R.X. Yang, A. Walsh and M.V. Kovalenko, *Nano letters*. **15**,3692 (2015).
- 3) J. Pospisil, O. Zmeskal, S. Nespurek, J. Krajcovic, M. Weiter and A. Kovalenko, *Scientific reports*. **9**,1 (2019).
- 4) Y. Wei, Z. Cheng and J. Lin, *Chemical Society Reviews*. **48**,310 (2019).
- 5) Y. Wu, X. Li and H. Zeng, *ACS Energy Letters*. **4**,673 (2019).
- 6) M. Zhang, Z.-Q. Tian, D.-L. Zhu, H. He, S.-W. Guo, Z.-L. Chen and D.-W. Pang, *New Journal of Chemistry*. **42**,9496 (2018).
- 7) J. Song, J. Li, X. Li, L. Xu, Y. Dong and H. Zeng, *Advanced materials*. **27**,7162 (2015).
- 8) J. Li, X. Yuan, P. Jing, J. Li, M. Wei, J. Hua, J. Zhao and L. Tian, *RSC advances*. **6**,78311 (2016).
- 9) B.A. Koscher, J.K. Swabeck, N.D. Bronstein and A.P. Alivisatos, *Journal of the American Chemical Society*. **139**,6566 (2017).
- 10) S. Chen, Y. Zhang, X. Zhang, J. Zhao, Z. Zhao, X. Su, Z. Hua, J. Zhang, J. Cao and J. Feng, *Advanced Materials*. **32**,2001107 (2020).
- 11) J. Zhang, C. Wang, X. Shen, M. Lu, J. Guo, X. Bai, Y. Zhang and W.W. Yu, *Applied Physics Letters*. **115**,193104 (2019).
- 12) F. Zhang, J. Song, B. Han, T. Fang, J. Li and H. Zeng, *Small Methods*. **2**,1700382 (2018).

- 13) Y. Dong, Y.-K. Wang, F. Yuan, A. Johnston, Y. Liu, D. Ma, M.-J. Choi, B. Chen, M. Chekini and S.-W. Baek, *Nature Nanotechnology*. **15**,668 (2020).
- 14) Y. Zhou and Y. Zhao, *Energy & Environmental Science*. **12**,1495 (2019).
- 15) Y. Zhou, J. Chen, O.M. Bakr and H.-T. Sun, *Chemistry of Materials*. **30**,6589 (2018).
- 16) S. Li, Z. Shi, F. Zhang, L. Wang, Z. Ma, D. Yang, Z. Yao, D. Wu, T.-T. Xu and Y. Tian, *Chemistry of Materials*. **31**,3917 (2019).
- 17) J.Y. Woo, Y. Kim, J. Bae, T.G. Kim, J.W. Kim, D.C. Lee and S. Jeong, *Chemistry of Materials*. **29**,7088 (2017).
- 18) F. Zhang, Z.-F. Shi, Z.-Z. Ma, Y. Li, S. Li, D. Wu, T.-T. Xu, X.-J. Li, C.-X. Shan and G.-T. Du, *Nanoscale*. **10**,20131 (2018).
- 19) M. Meyns, M. Perálvarez, A. Heuer-Jungemann, W. Hertog, M. Ibáñez, R. Nafria, A. Genç, J. Arbiol, M.V. Kovalenko and J. Carreras, *ACS applied materials & interfaces*. **8**,19579 (2016).
- 20) H. Wu, S. Wang, F. Cao, J. Zhou, Q. Wu, H. Wang, X. Li, L. Yin and X. Yang, *Chemistry of Materials*. **31**,1936 (2019).
- 21) D.H. Park, J.S. Han, W. Kim and H.S. Jang, *Dyes and Pigments*. **149**,246 (2018).
- 22) W. Chen, T. Shi, J. Du, Z. Zang, Z. Yao, M. Li, K. Sun, W. Hu, Y. Leng and X. Tang, *ACS applied materials & interfaces*. **10**,43978 (2018).
- 23) S.D. Liu and T.M. Chen, *Journal of the Chinese Chemical Society*. **67**,109 (2020).
- 24) B.R. Vale, E. Socie, A. Burgos-Caminal, J. Bettini, M.A. Schiavon and J.-E. Moser, *The Journal of Physical Chemistry Letters*. **11**,387 (2019).
- 25) N. Mondal and A. Samanta, *Nanoscale*. **9**,1878 (2017).
- 26) J. Chen, M.E. Messing, K. Zheng and T. Pullerits, *Journal of the American Chemical Society*. **141**,3532 (2019).
- 27) Y. Wu, C. Wei, X. Li, Y. Li, S. Qiu, W. Shen, B. Cai, Z. Sun, D. Yang and Z. Deng, *ACS Energy Letters*. **3**,2030 (2018).
- 28) J.B. Hoffman, A.L. Schleper and P.V. Kamat, *Journal of the American Chemical Society*. **138**,8603 (2016).
- 29) A. Buin, P. Pietsch, J. Xu, O. Voznyy, A.H. Ip, R. Comin and E.H. Sargent, *Nano letters*. **14**,6281 (2014).
- 30) V.K. Ravi, G.B. Markad and A. Nag, *ACS Energy Letters*. **1**,665 (2016).